**Supplemental Information**

# MAOA is essential for prostate tumorigenesis and cancer metastasis

**Jason Boyang Wu, Chen Shao, Xiangyan Li, Qinlong Li, Peizhen Hu, Changhong Shi, Yang Li, Yi-Ting Chen, Fei Yin, Chun-Peng Liao, Bangyan L. Stiles, Haiyen E. Zhau, Jean C. Shih and Leland W. K. Chung**

**Supplemental Data**

**Supplemental Figures 1, 2 and 3, related to Figure 1**

**Supplemental Figure 4, related to Figures 1, 2 and 4**

**Supplemental Figure 5, related to Figures 2 and 3**

**Supplemental Figures 6, 7 and 8, related to Figure 3**

**Supplemental Figures 9, 10 and 11, related to Figure 4**

**Supplemental Figure 12, related to Figure 5**

**Supplemental Figures 13, 14 and 15, related to Figure 6**

**Supplemental Figures 16-20**

**Supplemental Figure 21, related to Figures 1-5**

**Supplemental Table 1, related to Figures 6, 7 and Supplemental Figure 4**

**Supplemental Table 2, related to Figure 8**

**Supplemental Tables 3 and 4, related to Figure 10**

**Supplemental Methods**

**Supplemental References**

**Supplemental Figure 1**

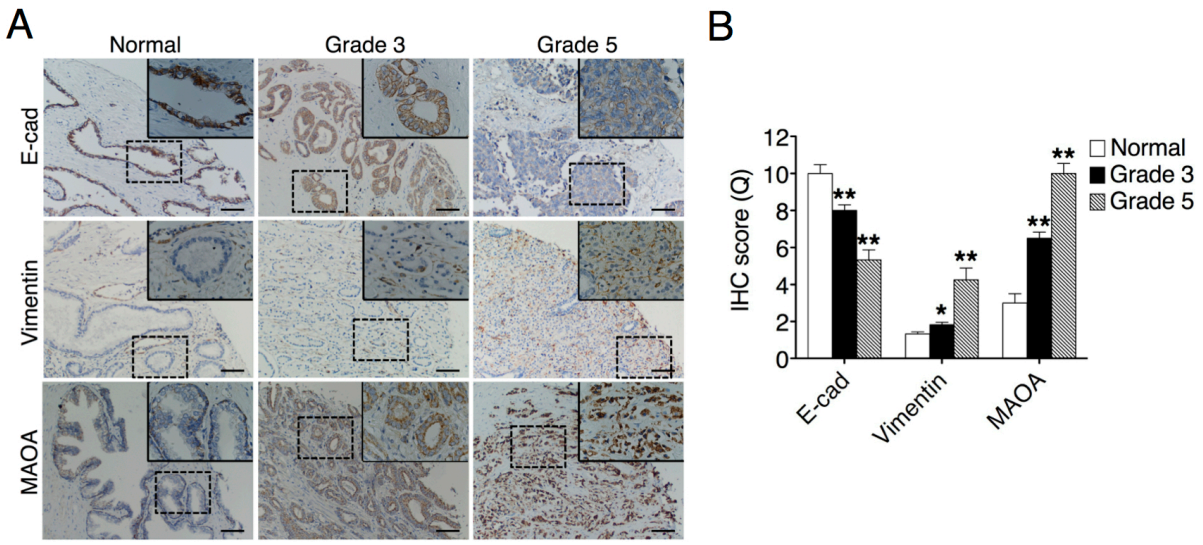


**Supplemental Figure 1**
MAOA and EMT in PCa. (**A**) Representative IHC images of normal prostatic epithelium and Gleason grade 3 and 5 PCa specimens stained for E-cadherin, Vimentin and MAOA from a clinical tissue microarray comprising 40 prostate adenocarcinomas and 9 adjacent normal tissue. The enlargement of representative areas indicated in dashed rectangles is shown. Original magnification, x100; scale bars represent 40 μm. (**B**) Semi-quantitative analysis of IHC staining for E-cadherin, Vimentin and MAOA (N=9, 22 and 18 for normal, G3 and G5, respectively). Data represent the mean ± SEM. Detailed quantitative methodology is given in Supplemental Methods. * $p<0.05$, ** $p<0.01$.

**Supplemental Figure 2**

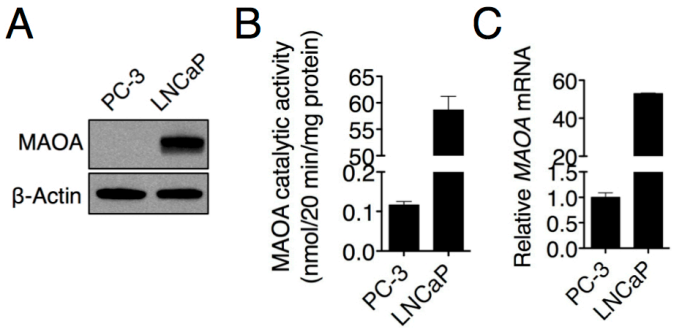


**Supplemental Figure 2**
MAOA expression in PC-3 and LNCaP cells. (**A**) Immunoblots of PC-3 and LNCaP cells for MAOA. (**B**) Determination of MAOA enzymatic activity (mean ± SEM, N=3) in PC-3 and LNCaP cells. (**C**) qPCR analysis of *MAOA* mRNA expression (mean ± SEM, N=3) in PC-3 and LNCaP cells.

**Supplemental Figure 3**

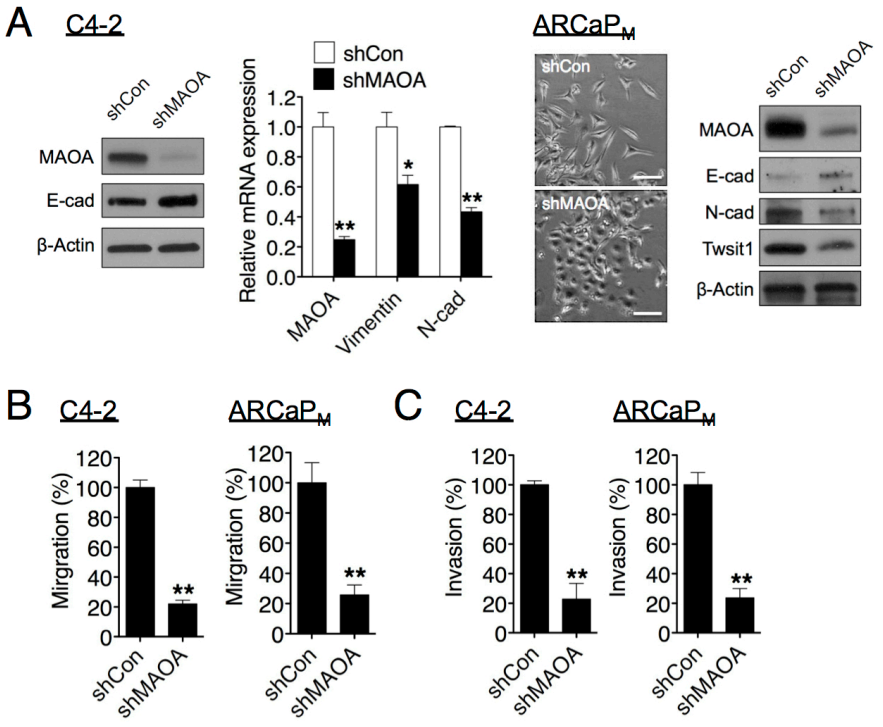


**Supplemental Figure 3**

MAOA and EMT in PCa. (**A**) Immunoblots of C4-2 and ARCaP$_M$ cells that express a *MAOA*-targeting shRNA (shMAOA) or a scrambled shRNA (shCon) for EMT marker protein expression. The mRNA expression (mean ± SEM, N=3) of *MAOA*, *Vimentin* and *N-cadherin* in paired C4-2 cells was measured by qPCR. ARCaP$_M$ (shCon and shMAOA) cell morphology was photographed. Original magnification, x40; scale bars represent 200 µm. * $p$<0.05, ** $p$<0.01. (**B, C**) C4-2 and ARCaP$_M$ (shCon and shMAOA) cells were assessed for their ability to either migrate (**B**) or invade (**C**). The migration or invasion of respective control cells was set as 100%. Data represent the mean ± SEM of three separate experiments. ** $p$<0.01.

**Supplemental Figure 4**

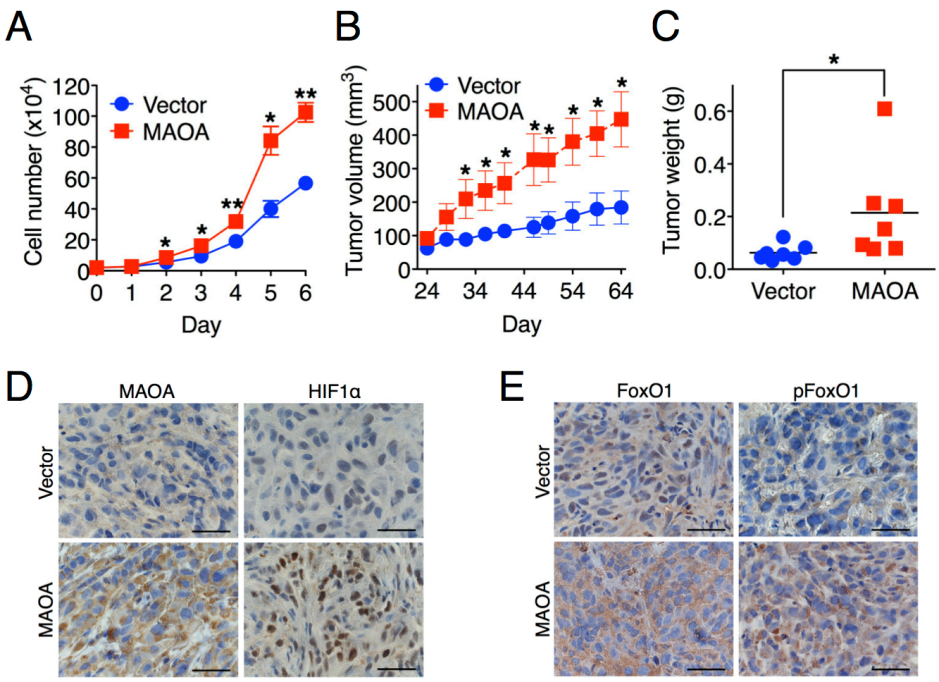


**Supplemental Figure 4**

Overexpression of MAOA increased the growth of PC-3 cells and tumor xenografts. (**A**) Growth curves of stable control and MAOA-overexpressing PC-3 cells cultured in standard media. 2 x $10^4$ cells were seeded initially followed by cell number count over 6 consecutive days. Data represent the mean ± SEM of three experiments. (**B, C**) PC-3 cells that stably express an empty vector or a *MAOA* expression construct were subcutaneously injected into male nude mice (N=5 mice for each group with 2 tumors implanted initially per mouse) to allow the growth of tumor xenografts. Tumor growth was determined by measuring tumor volume and tumor weight. The graph shows the mean (±SEM) tumor size at the indicated time * $p<0.05$, ** $p<0.01$. (**D, E**) IHC analysis of tumor samples for MAOA, HIF1α (**D**), FoxO1 and pFoxO1 (**E**) levels. Representative images are shown. Original magnification, x400; scale bars represent 20 μm.

**Supplemental Figure 5**

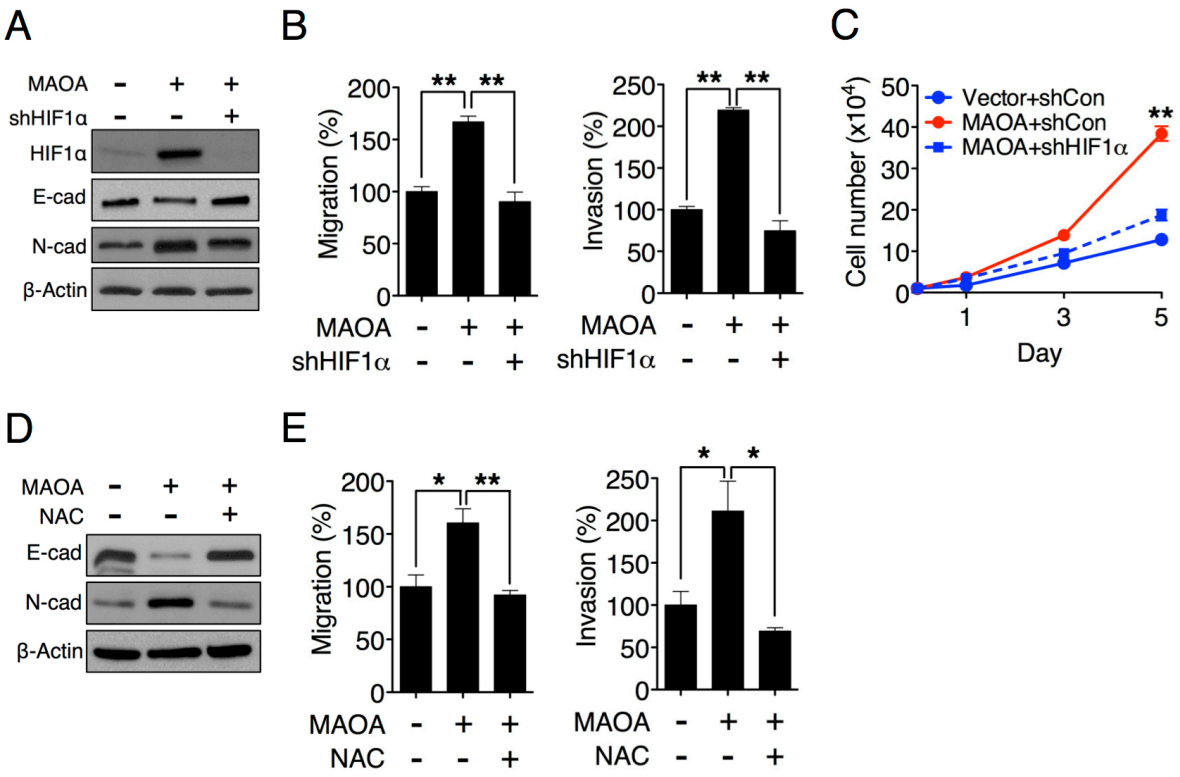


**Supplemental Figure 5**
Effects of HIF1α and ROS on MAOA-mediated EMT. (**A**) Immunoblots of different stable PC-3 cells as indicated for EMT marker protein expression. shHIF1α indicates *HIF1α*-targeting shRNAs used to knock down *HIF1α* gene expression. (**B**) Different PC-3 cells as established in (**A**) were assessed for their ability to either migrate (left) or invade (right). The migration or invasion of control cells was set as 100%. Data represent the mean ± SEM of three separate experiments. ** $p<0.01$. (**C**) Growth curves of PC-3 cells as established in (**A**). 1 x $10^4$ cells were seeded initially followed by cell number count over 5 consecutive days. Data represent the mean ± SEM of three separate experiments. ** $p<0.01$. (**D**) Immunoblots of PC-3 (vector and MAOA-overexpression) cells treated with or without NAC (10 mM, 48 hr) as indicated for EMT marker expression. (**E**) PC-3 cells (vector and MAOA-overexpression) pre-treated with or without NAC (10 mM, 24 hr) were assessed for the ability to either migrate (left) or invade (right). The migration or invasion of control cells was set as 100%. Data represent the mean ± SEM of three separate experiments. * $p<0.05$, ** $p<0.01$.

**Supplemental Figure 6**

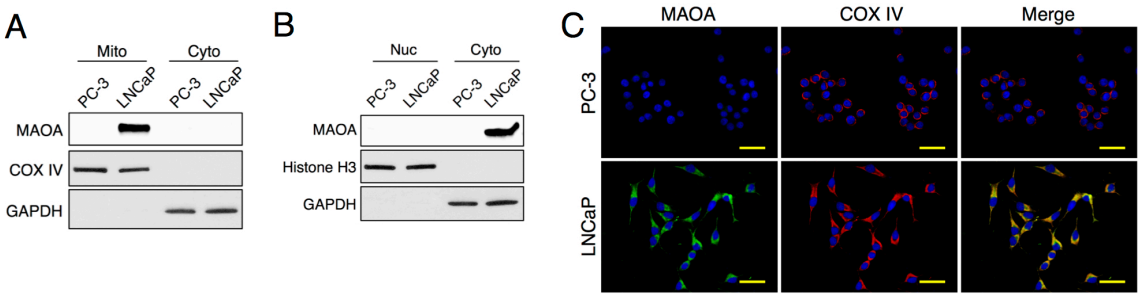


**Supplemental Figure 6**

MAOA localization in PCa cells. (**A**) Immunoblots of mitochondrial and cytoplasmic fractions of PC-3 (MAOA-negative) and LNCaP (MAOA-positive) cells for MAOA. COX IV and GAPDH serve as mitochondrial and cytoplasmic markers, respectively. (**B**) Immunoblots of nuclear and cytoplasmic fractions of PC-3 and LNCaP cells for MAOA. Histone H3 and GAPDH serve as nuclear and cytoplasmic markers, respectively. (**C**) Immunofluorescence analysis of MAOA (green) in PC-3 and LNCaP cells. COX IV (red) and DAPI (blue) serve as markers for mitochondria and nuclei, respectively. Representative images are shown. Original magnification, x400; scale bars represent 20 μm.

**Supplemental Figure 7**

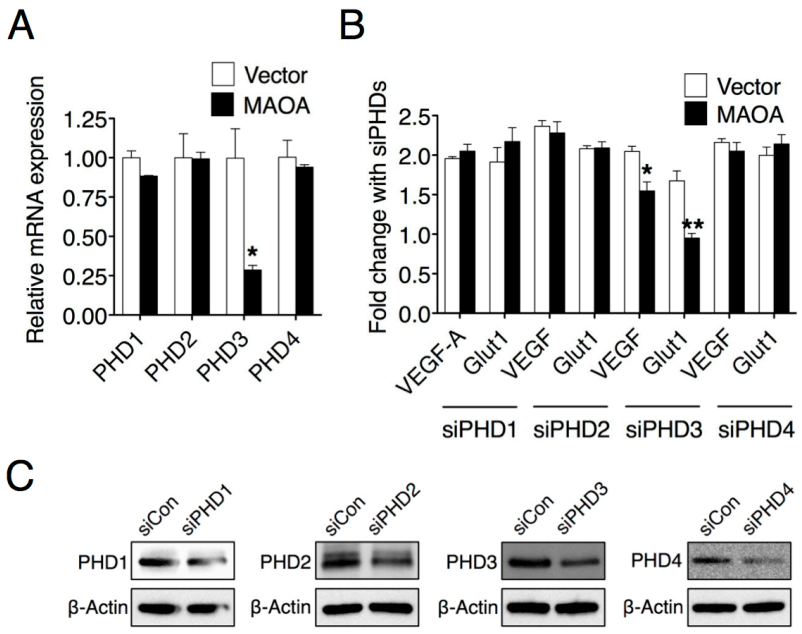


**Supplemental Figure 7**
MAOA regulates PHDs for mediating hypoxic effects. (**A**) qPCR analysis of PC-3 (vector and MAOA-overexpression) cells for the mRNA expression (mean ± SEM, N=3) of 4 isoforms of *PHD*. * $p<0.05$. (**B**) Fold induction of HIF1α target genes in PC-3 (vector and MAOA-overexpression) cells transiently transfected with either control siRNA or siRNAs specifically targeting *PHD1-4* was measured by qPCR, and the ratio (mean ± SEM, N=3) of PHD-knockdown to control gene expression is shown. * $p<0.05$, ** $p<0.01$. (**C**) Immunoblots of PC-3 cells as used in (**B**) for confirming the knockdown efficacy of various PHDs. Representative blots of vector-expressing PC-3 cells are shown.

**Supplemental Figure 8**

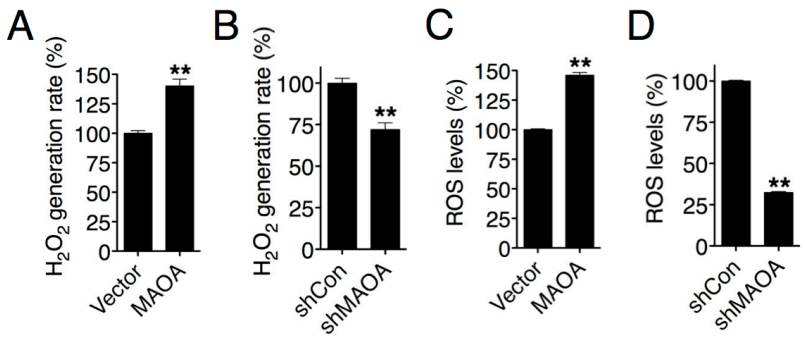


**Supplemental Figure 8**
MAOA induces ROS. (**A, B**) Determination of $H_2O_2$ generation rate in intact mitochondria isolated from PC-3 (vector and MAOA-overexpressing) (**A**) or LNCaP (shCon and shMAOA) (**B**) cells by AmplexRed Hydrogen Peroxide Assay Kit. The rate in control cells was set as 100%. Data represent the mean ± SEM of three experiments. ** $p$<0.01. (**C, D**) Determination of cellular general ROS levels in paired PC-3 (**C**) or LNCaP (**D**) cells by incubating cells with a ROS-sensitive dye (CM-$H_2$DCFDA) followed by FACS analysis. ROS levels in control cells were set as 100%. Data represent the mean ± SEM of three experiments. ** $p$<0.01.

**Supplemental Figure 9**

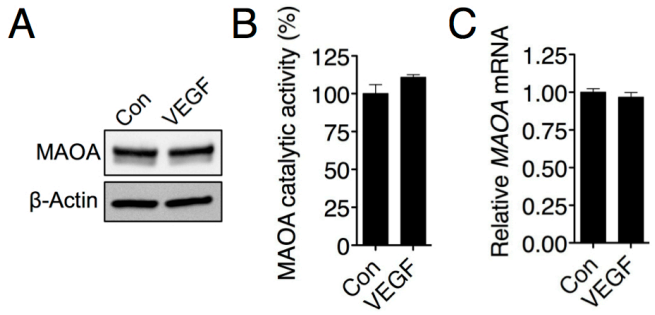


**Supplemental Figure 9**
VEGF effects on MAOA. (**A**) Immunoblots of LNCaP cells treated with or without recombinant $VEGF_{165}$ (50 ng/ml, 48 hr) for MAOA. (**B**) Determination of MAOA enzymatic activity (mean ± SEM, N=3) in LNCaP cells as used in (**A**). (**C**) qPCR analysis of *MAOA* mRNA expression (mean ± SEM, N=3) in LNCaP cells treated with or without recombinant $VEGF_{165}$ (50 ng/ml, 24 hr).

**Supplemental Figure 10**

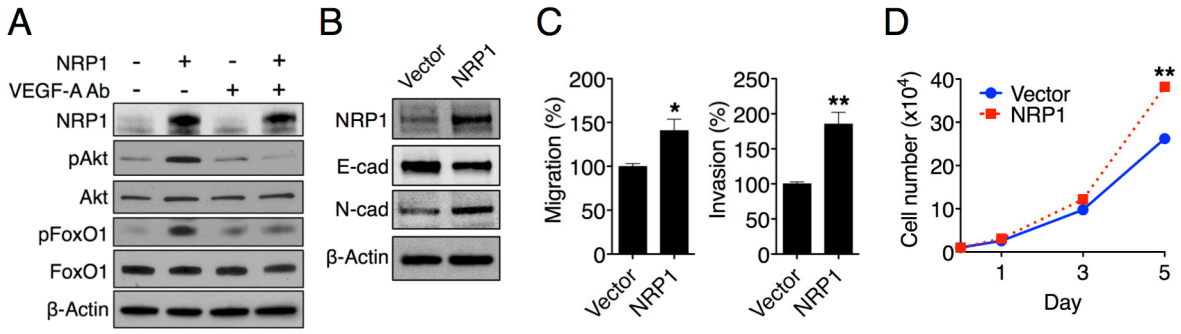


**Supplemental Figure 10**

NRP1 effects on EMT. (**A**) Immunoblots of PC-3 (vector and NRP1-overexpression) cells treated with either anti-VEGF-A antibody or control IgG (0.5 μg/ml, 24 hr) for NRP1, pAkt (Ser473) and pFoxO1 (Thr24). (**B**) Immunoblots of PC-3 (vector and NRP1-overexpression) cells for EMT marker protein expression. (**C**) PC-3 (vector and NRP1-overexpression) cells were assessed for their ability to either migrate (left) or invade (right). The migration or invasion of control cells was set as 100%. Data represent the mean ± SEM of three separate experiments. * $p<0.05$, ** $p<0.01$. (**D**) Growth curves of PC-3 (vector and NRP1-overexpression) cells. 1 x $10^4$ cells were seeded initially followed by cell number count over 5 consecutive days. Data represent the mean ± SEM of three separate experiments. ** $p<0.01$.

**Supplemental Figure 11**

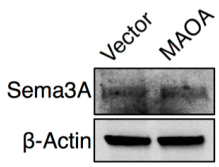


**Supplemental Figure 11**
Immunoblots of PC-3 (vector and MAOA-overexpression) cells for Sema3A.

**Supplemental Figure 12**

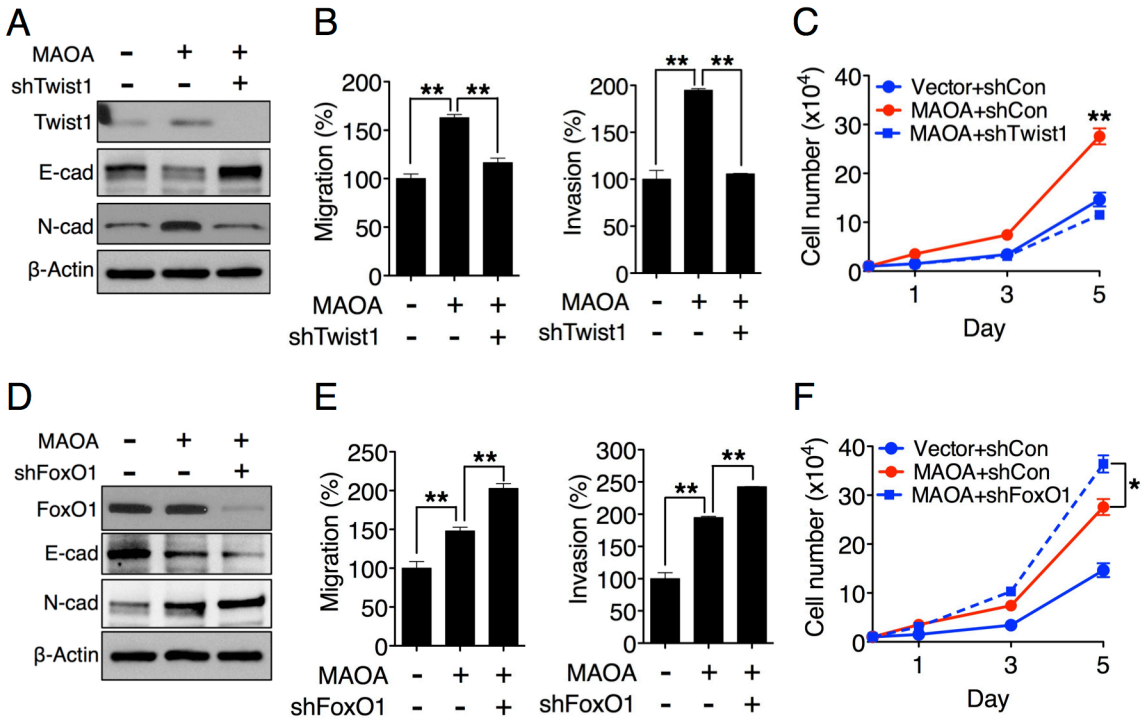


**Supplemental Figure 12**
Effects of Twist1 and FoxO1 on MAOA-mediated EMT. (**A, D**) Immunoblots of different stable PC-3 cells as indicated for EMT marker protein expression. shTwist1 and shFoxO1 indicate *Twist1*- and *FoxO1*-targeting shRNAs respecitvely. (**B, E**) Different PC-3 cells as established in (**A**) or (**D**) were assessed for their ability to either migrate (left) or invade (right). The migration or invasion of control cells was set as 100%. Data represent the mean ± SEM of three separate experiments. ** $p<0.01$. (**C, F**) Growth curves of PC-3 cells as established in (**A**) or (**D**). 1 x $10^4$ cells were seeded initially followed by cell number count over 5 consecutive days. Data represent the mean ± SEM of three separate experiments. * $p<0.05$, ** $p<0.01$.

**Supplemental Figure 13**

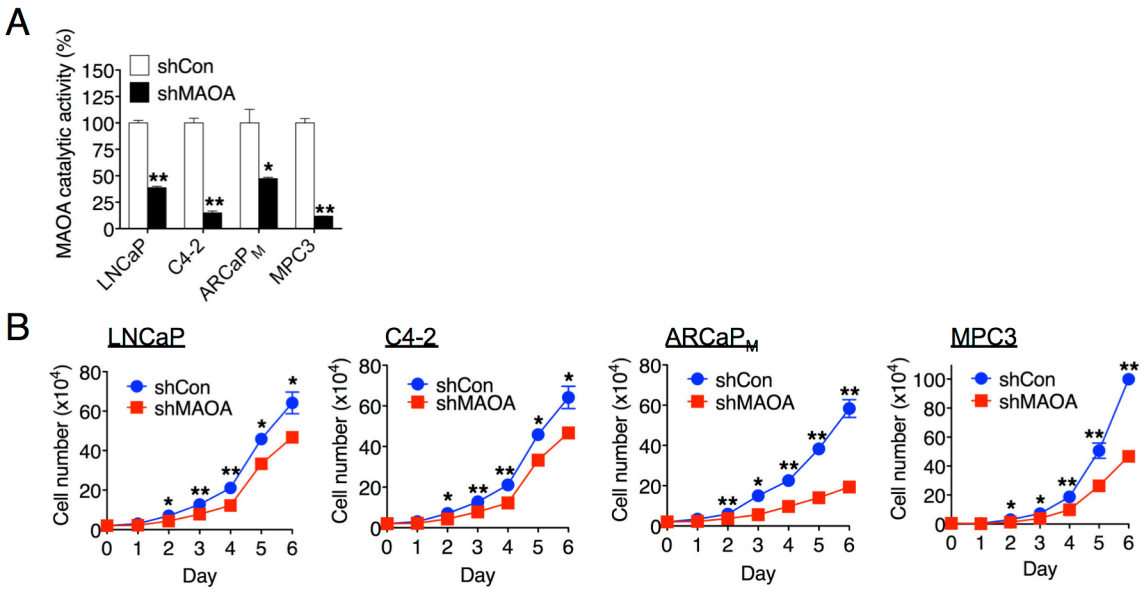


**Supplemental Figure 13**

MAOA knockdown reduced PCa cell proliferation. (**A**) Determination of the efficacy of MAOA knockdown in human PCa LNCaP, C4-2 and $ARCaP_M$ and murine PCa MPC3 (shCon and shMAOA) cells by MAOA enzymatic activity assay. MAOA activity in control cells was set as 100%. Data represent the mean ± SEM of three separate experiments. * $p<0.05$, ** $p<0.01$. (**B**) Growth curves of paired LNCaP, C4-2, $ARCaP_M$ and MPC3 (shCon and shMAOA) cells cultured in standard media. 2 x $10^4$ cells were seeded initially followed by cell number count over 6 consecutive days. Data represent the mean ± SEM of three separate experiments. * $p<0.05$, ** $p<0.01$.

**Supplemental Figure 14**

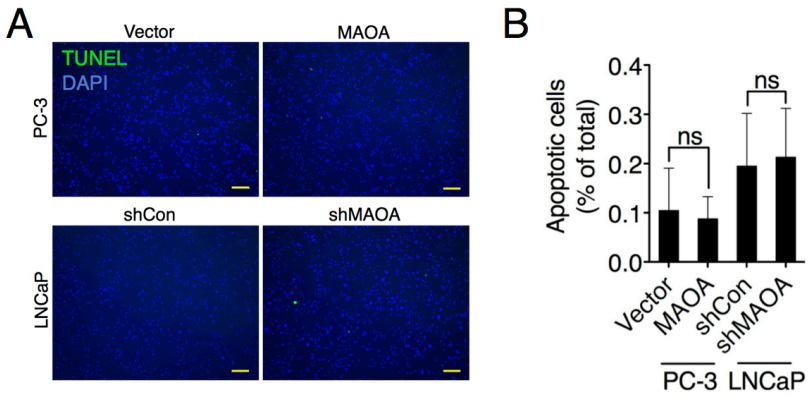


**Supplemental Figure 14**
MAOA effects on apoptosis. (**A**) Representative images of apoptosis of PC-3 (vector and MAOA-overexpression) and LNCaP (shCon and shMAOA) cells analyzed by TUNEL assay. Original magnification, x100; scale bars represent 10 μm. (**B**) Quantification of apoptosis of cells (N=5) in (**A**). Data represent the mean ± SEM of three separate experiments. Ns, not significant.

**Supplemental Figure 15**

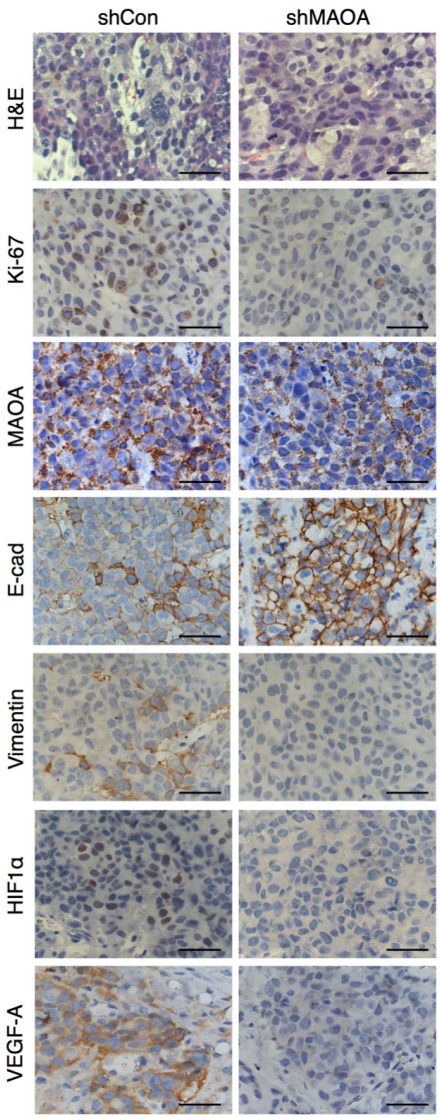


**Supplemental Figure 15**
**H**&E and IHC analysis of Ki-67, MAOA, E-cadherin, Vimentin, HIF1α and VEGF-A expression in C4-2 (shCon and shMAOA) tumor xenografts. Representative images from five separate samples are shown. Original magnification, x400; scale bars represent 20 μm.

**Supplemental Figure 16**

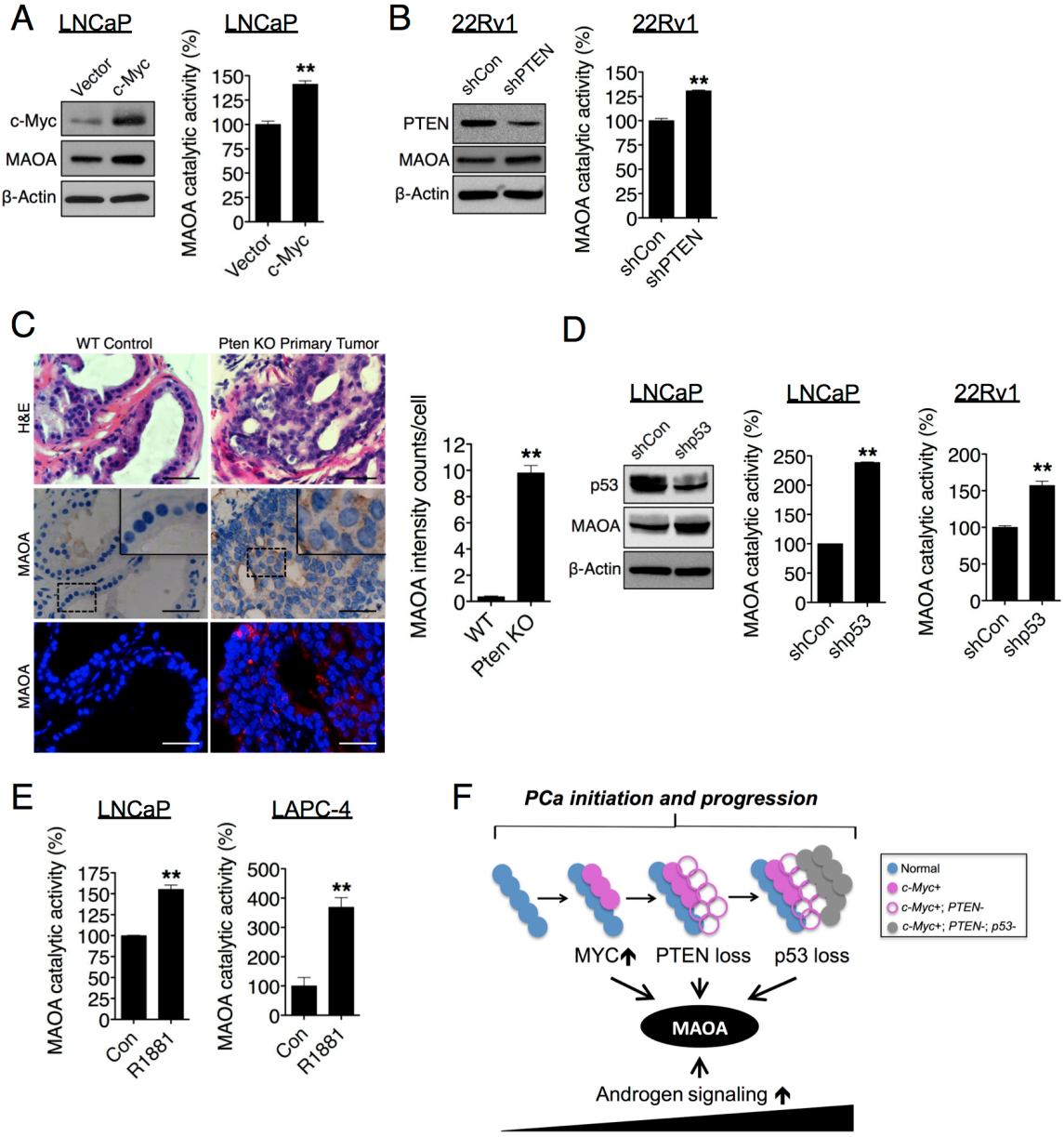


**Supplemental Figure 16**

Induction of MAOA in PCa. (**A**) Determination of MAOA protein expression (left) and enzymatic activity (mean ± SEM, N=3, right) in LNCaP cells that stably express either a *c-Myc* construct or an empty vector. ** $p<0.01$. (**B**) Determination of MAOA protein expression (left) and enzymatic activity (mean ± SEM, N=3, right) in 22Rv1 (with wild-type PTEN) cells that stably express either *PTEN*-targeting shRNAs or a scrambled shRNA. ** $p<0.01$. (**C**) H&E, IHC and single quantum dot labeling analysis of normal (WT) and neoplastic (9-month-old prostate-specific *Pten*-KO primary tumor) mouse epithelium of the dorsolateral prostatic lobes for MAOA protein expression (left). Original magnification, x400; scale bars represent 20 μm. Cell-based average intensity counts

(mean ± SEM) from 1,000 each of normal and neoplastic samples were quantified using inForm software (right). ** $p<0.01$. (**D**) Determination of MAOA protein expression (left) and enzymatic activity (mean ± SEM, N=3, middle and right) in LNCaP and 22Rv1 (both with wild-type p53) cells that stably express either *p53*-targeting shRNAs or a scrambled shRNA. ** $p<0.01$. (**E**) Determination of MAOA enzymatic activity (mean ± SEM, N=3) in LNCaP and LAPC-4 (both androgen-responsive) cells treated with either R1881 (10 nM, 24 hr) or vehicle (ethanol). ** $p<0.01$. (**F**) A schematic diagram summarizing the potential cues, including c-Myc overexpression, the loss of PTEN and p53 as well as activated androgen signaling, to coordinately contribute to the upregulation of MAOA in PCa.

**Supplemental Figure 17**

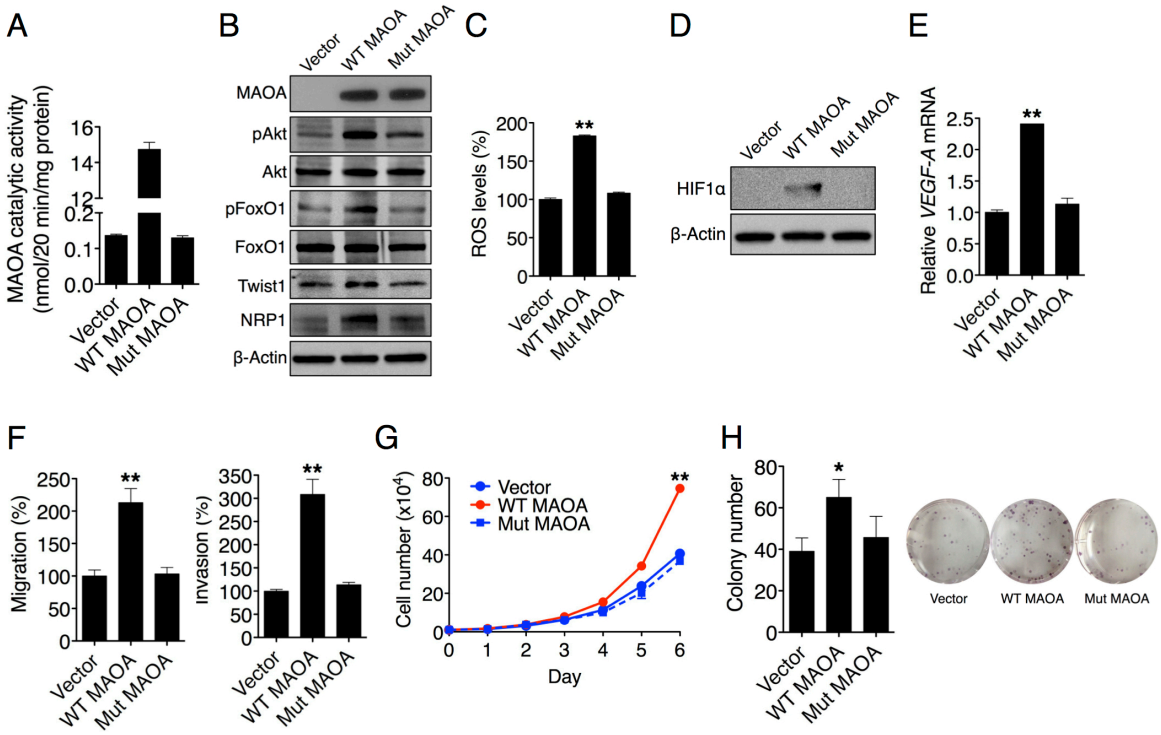


**Supplemental Figure 17**

MAOA enzymatic activity dominates its function in PCa. (**A**) Determination of MAOA enzymatic activity (mean ± SEM, N=3) in PC-3 cells that stably overexpress an empty vector (Vector), a wild-type (WT) *MAOA* expression construct, or a mutated (Mut) *MAOA* expression construct that is defective in enzymatic activity but with intact protein expression. (**B**) Immunoblots of the different stable PC-3 cells as indicated for pAkt (Ser473), pFoxO1 (Thr24), Twist1 and NRP1. (**C**) Determination of ROS levels (mean ± SEM, N=3) in the different stable PC-3 cells. ** $p$<0.01. (**D**) Immunoblots of the different stable PC-3 cells under hypoxia (1% $O_2$, 24 hr) for HIF1α. (**E**) qPCR analysis of the different stable PC-3 cells for *VEGF-A* mRNA expression (mean ± SEM, N=3). ** $p$<0.01. (**F**) Different stable PC-3 cells were assessed for their ability to either migrate (left) or invade (right). The migration or invasion of vector-expressing cells was set as 100%. Data represent the mean ± SEM of three separate experiments. ** $p$<0.01. (**G**) Growth curves of the different stable PC-3 cells. 1 x $10^4$ cells were seeded initially followed by cell number count over 6 consecutive days. Data represent the mean ± SEM of three separate experiments. ** $p$<0.01. (**H**) Different stable PC-3 cells were assessed for their ability to form colonies in vitro. 100 cells were seeded initially prior to 2-week culture, and the colonies formed were stained by crystal violet (right) and the numbers (mean ± SEM, N=3) were counted (left). * $p$<0.05.

**Supplemental Figure 18**

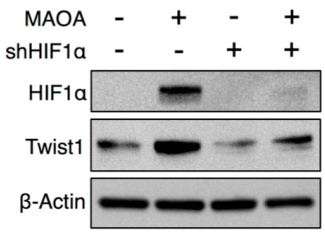


**Supplemental Figure 18**
Immunoblots of PC-3 (vector and MAOA-overexpression) cells with or without stable knockdown of HIF1α for Twist1. shHIF1α indicates *HIF1α*-targeting shRNAs.

**Supplemental Figure 19**

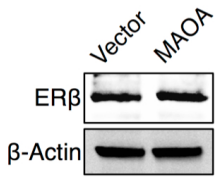


**Supplemental Figure 19**
Immunoblots of PC-3 (vector and MAOA-overexpression) cells for ERβ protein expression.

**Supplemental Figure 20**

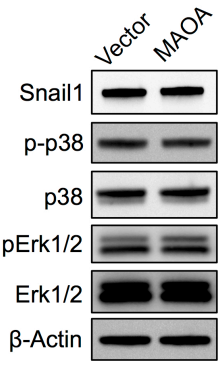


**Supplemental Figure 20**
Immunoblots of PC-3 (vector and MAOA-overexpression) cells for Snail1, p-p38 and pErk1/2 expression.

## Supplemental Figure 21

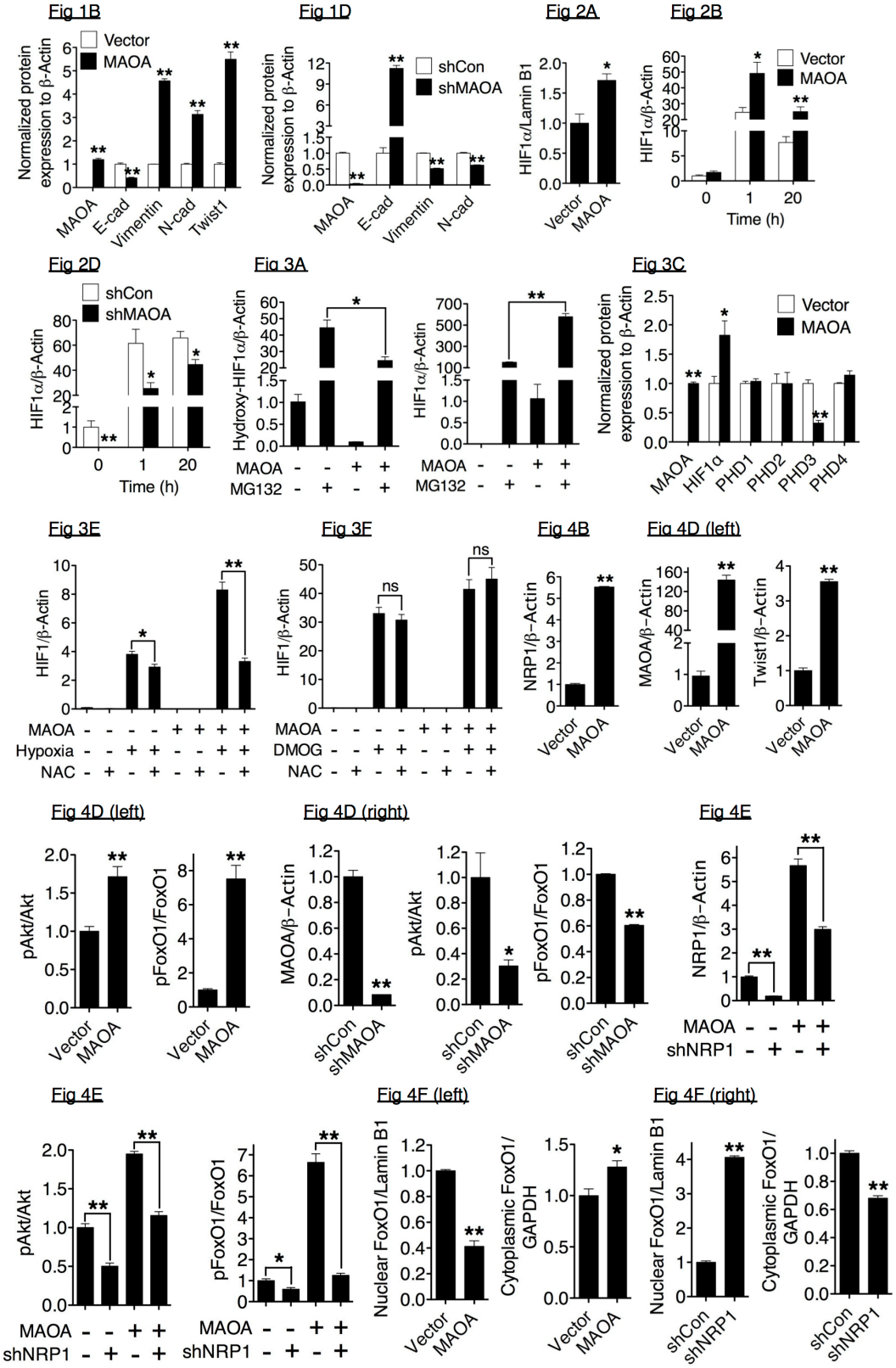

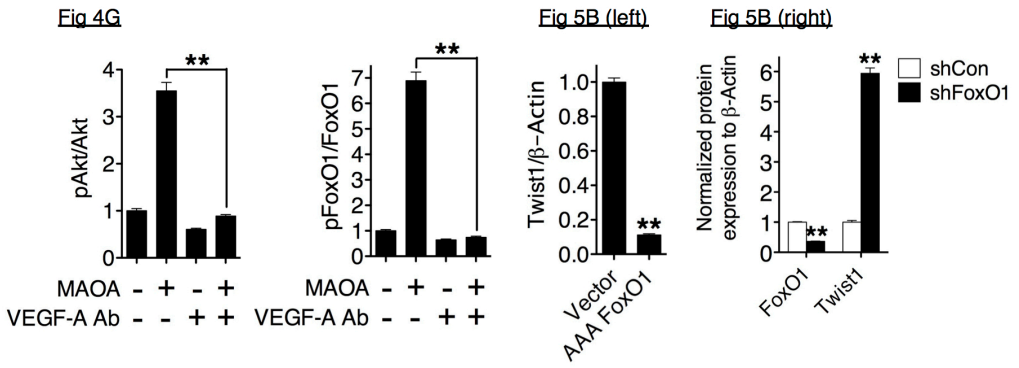


**Supplemental Figure 21**
Morphometric analysis of immunoblots in Figures 1-11 by ImageJ. (mean ± SEM, N=3). Raito of target protein expression normalized to different loading controls as indicated is presented, and the ratio in control cell groups is arbitrarily set as 1. * $p$<0.05, ** $p$<0.01.

**Supplemental Table 1**

| Cells | Mice/group | Tumors/mouse | Expected number of tumors | Actual number of tumors |
|---|---|---|---|---|
| LNCaP shCon | 5 | 2 | 10 | 10 |
| LNCaP shMAOA | 5 | 2 | 10 | 10 |
| C4-2 shCon | 6 | 2 | 12 | 12 |
| C4-2 shMAOA | 6 | 2 | 12 | 5 |
| $ARCaP_M$ shCon | 4 | 2 | 8 | 8 |
| $ARCaP_M$ shMAOA | 4 | 2 | 8 | 0 |
| MPC3 shCon | 6 | 2 | 12 | 12 |
| MPC3 shMAOA | 6 | 2 | 12 | 0 |
| C4-2 Con | 5 | 1 | 5 | 5 |
| C4-2 Clorgyline | 5 | 1 | 5 | 5 |
| PC-3 Vector | 10 | 1 | 10 | 7 |
| PC-3 MAOA | 10 | 1 | 10 | 7 |

**Supplemental Table 1**
Summary of the number of mice and tumor injections used for establishing subcutaneous tumor xenograft mouse models in the present study (referring to Figures 6 and 7 and Supplemental Figure 4).

**Supplemental Table 2**

| | Bone (limbs, ribs, jaw) | Adrenal gland | Lymph node | Lung | Liver |
|---|---|---|---|---|---|
| shCon | 10/10 (100%) | 7/10 (70%) | 7/10 (70%) | 5/10 (50%) | 6/10 (60%) |
| shMAOA | 1/10 (10%) | 0/10 (0%) | 0/10 (0%) | 2/10 (20%) | 0/10 (0%) |

**Supplemental Table 2**
Summary of metastatic sites of control (shCon) and MAOA-knockdown (shMAOA) $ARCaP_M$ cells at mouse necropsy in Week 10 (N=10 mice for each group).

**Supplemental Table 3**

| No. | Sex | Age | Pathological diagnosis | Gleason score | TNM | Stage | MAOA |
|---|---|---|---|---|---|---|---|
| 1 | M | 70 | Adenocarcinoma | 8 | T3bN0M0 | III | + |
| 2 | M | 72 | Adenocarcinoma | 7 | T3bN0M0 | III | ++ |
| 3 | M | 63 | Adenocarcinoma | 10 | T3bN0M0 | III | ++ |
| 4 | M | 62 | Adenocarcinoma | 9 | T3bN0M0 | III | ++ |
| 5 | M | 73 | Adenocarcinoma | 8 | T3bN0M0 | III | ++ |
| 6 | M | 68 | Adenocarcinoma | 8 | T3bN0M0 | III | ++ |
| 7 | M | 70 | Adenocarcinoma | 6 | T3bN0M0 | III | + |
| 8 | M | 65 | Adenocarcinoma | 7 | T2cN0M0 | II | +++ |
| 9 | M | 72 | Adenocarcinoma | 9 | T3bN0M0 | III | ++ |
| 10 | M | 66 | Adenocarcinoma | 8 | T3bN0M0 | III | ++ |
| 11 | M | 59 | Adenocarcinoma | 6 | T2bN0M0 | II | ++ |
| 12 | M | 58 | Adenocarcinoma | 9 | T3bN0M0 | III | + |
| 13 | M | 70 | Adenocarcinoma | 7 | T3aN0M0 | III | +++ |
| 14 | M | 63 | Adenocarcinoma | 9 | T3bN0M0 | III | + |
| 15 | M | 62 | Adenocarcinoma | 9 | T3bN0M0 | III | ++ |
| 16 | M | 69 | Adenocarcinoma | 7 | T3aN0M0 | III | + |
| 17 | M | 69 | Adenocarcinoma | 7 | T3bN0M0 | III | ++ |
| 18 | M | 61 | Adenocarcinoma | 9 | T3bN0M0 | III | +++ |
| 19 | M | 63 | Adenocarcinoma | 9 | T3aN1M0 | III | +++ |
| 20 | M | 67 | Adenocarcinoma | 9 | T3bN1M0 | III | ++ |
| 21 | M | 70 | Adenocarcinoma | 7 | T3bN0M0 | III | +++ |
| 22 | M | 60 | Adenocarcinoma | 9 | T3bN0M0 | III | + |
| 23 | M | 76 | Adenocarcinoma | 7 | T2cN0M0 | II | ++ |
| 24 | M | 62 | Adenocarcinoma | 7 | T2cN0M1 | II | ++ |
| 25 | M | 68 | Adenocarcinoma | 8 | T4N0M0 | IV | ++ |
| 26 | M | 66 | Adenocarcinoma | 7 | T3aN0M0 | III | +++ |
| 27 | M | 66 | Adenocarcinoma | 9 | T3bN0M0 | III | +++ |
| 28 | M | 73 | Adenocarcinoma | 7 | T2cN0M0 | II | + |
| 29 | M | 67 | Adenocarcinoma | 10 | T3aN0M0 | III | ++ |
| 30 | M | 69 | Adenocarcinoma | 7 | T2cN0M0 | II | +++ |
| 31 | M | 65 | Adenocarcinoma | 8 | T3bN0M0 | III | ++ |
| 32 | M | 64 | Adenocarcinoma | 7 | T2cN0M0 | II | ++ |
| 33 | M | 59 | Adenocarcinoma | 9 | T3bN0M0 | III | ++ |
| 34 | M | 64 | Adenocarcinoma | 10 | T3aN0M0 | III | ++ |
| 35 | M | 71 | Adenocarcinoma | 9 | T3bN0M0 | III | +++ |
| 36 | M | 67 | Adenocarcinoma | 7 | T2cN0M0 | II | ++ |
| 37 | M | 60 | Adenocarcinoma | 9 | T3bN0M0 | III | ++ |
| 38 | M | 44 | Adenocarcinoma | 7 | T3bN0M0 | III | +++ |
| 39 | M | 75 | Adenocarcinoma | 8 | T2cN0M0 | III | +++ |
| 40 | M | 78 | Adenocarcinoma | 9 | T3bN0M0 | III | +++ |
| 41 | M | 53 | Adenocarcinoma | 9 | T3bN0M0 | III | +++ |
| 42 | M | 63 | Adenocarcinoma | 8 | T3bN0M0 | III | +++ |
| 43 | M | 63 | Adenocarcinoma | 9 | T3bN0M0 | III | +++ |
| 44 | M | 70 | Adenocarcinoma | 7 | T2cN0M0 | II | +++ |

| | | | | | | | |
|---|---|---|---|---|---|---|---|
| 45 | M | 57 | Adenocarcinoma | 7 | T3bN0M9 | III | +++ |
| 46 | M | 70 | Adenocarcinoma | 7 | T2cN0M1 | II | +++ |
| 47 | M | 71 | Adenocarcinoma | 8 | T3bN0M0 | III | +++ |
| 48 | M | 72 | Adenocarcinoma | 8 | T2cN0M0 | II | +++ |
| 49 | M | 68 | Adenocarcinoma | 8 | T3bN0M0 | III | +++ |
| 50 | M | 75 | Adenocarcinoma | 9 | T3bN0M0 | III | +++ |
| 51 | M | 67 | Adenocarcinoma | 9 | T3bN0M0 | III | +++ |
| 52 | M | 72 | Adenocarcinoma | 9 | T3bN0M0 | III | +++ |
| 53 | M | 63 | Adenocarcinoma | 9 | T3bN0M0 | III | +++ |
| 54 | M | 58 | Adenocarcinoma | 9 | T3bN0M0 | III | +++ |
| 55 | M | 69 | Adenocarcinoma | 8 | T3bN0M0 | III | +++ |
| 56 | M | 49 | Adenocarcinoma | 7 | T3bN0M1 | III | +++ |
| 57 | M | 64 | Adenocarcinoma | 6 | T2bN0M0 | II | +++ |
| 58 | M | 70 | Adenocarcinoma | 7 | T3bN0M0 | III | +++ |
| 59 | M | 65 | Adenocarcinoma | 9 | T3bN0M0 | III | +++ |
| 60 | M | 58 | Adenocarcinoma | 7 | T3bN0M0 | III | +++ |
| 61 | M | 71 | Adenocarcinoma | 7 | T2cN0M0 | II | +++ |
| 62 | M | 75 | Adenocarcinoma | 7 | T3aN0M1 | III | +++ |
| 63 | M | 66 | Adenocarcinoma | 9 | T3bN0M0 | III | +++ |
| 64 | M | 72 | Adenocarcinoma | 7 | T3aN0M1 | III | +++ |
| 65 | M | 73 | Adenocarcinoma | 7 | T3bN0M0 | III | +++ |
| 66 | M | 62 | Adenocarcinoma | 7 | T3bN0M0 | III | +++ |
| 67 | M | 72 | Adenocarcinoma | 9 | T3bN1M0 | IV | +++ |
| 68 | M | 75 | Adenocarcinoma | 7 | T4N0M0 | IV | +++ |
| 69 | M | 68 | Adenocarcinoma | 9 | T3bN0M0 | III | +++ |
| 70 | M | 68 | Adenocarcinoma | 9 | T3bN0M1 | III | +++ |
| 71 | M | 69 | Adenocarcinoma | 9 | T3bN0M0 | III | +++ |
| 62 | M | 76 | Adenocarcinoma | 7 | T2cN0M0 | II | +++ |
| 73 | M | 74 | Adenocarcinoma | 7 | T2cN0M1 | II | +++ |
| 74 | M | 76 | Adenocarcinoma | 9 | T3bN0M0 | III | +++ |

**Supplemental Table 3**
Clinical and pathological annotation of TMAs. Information on the patients' treatment history is not available.

**Supplemental Table 4**

| *MAOA* | | | *ERG* | | | Data | Sample | Refs. |
|---|---|---|---|---|---|---|---|---|
| **Score** | **Rank** | **%** | **Score** | **Rank** | **%** | **set** | **size** | |
| 13.3 | 8% | 95 | 6.8 | 1% | 95 | Taylor 3 | 185 | (1) |
| 8.2 | 2% | 90 | 6.3 | 1% | 75 | Varambally | 19 | (2) |
| 7.4 | 2% | 95 | 8.8 | 1% | 75 | Liu | 57 | (3) |
| 4.1 | 2% | 90 | 3.3 | 1% | 75 | Holzbeierlein | 54 | (4) |
| 4.5 | 13% | 95 | 2.7 | 1% | 75 | Yu | 112 | (5) |
| 4.0 | 4% | 95 | 6.7 | 1% | 90 | Tomlins | 101 | (6) |
| 4.0 | 7% | 90 | 1.1 | 43% | 75 | Best 2 | 20 | (7) |
| 3.9 | 4% | 90 | 1.4 | 14% | 75 | Tamura | 35 | (8) |
| 3.5 | 17% | 90 | 77.0 | 3% | 95 | Magee | 15 | (9) |
| 3.1 | 11% | 90 | 1.7 | 2% | 75 | Wallace | 89 | (10) |
| 3.0 | 11% | 90 | 3.5 | 1% | 75 | LaTuippe | 35 | (11) |
| 2.8 | 11% | 90 | 3.9 | 1% | 75 | Bittner | 60 | unpublished |
| 1.7 | 7% | 75 | 5.9 | 1% | 75 | Vanaja | 40 | (12) |
| 1.3 | 18% | 75 | 1.5 | 10% | 75 | Nanni | 30 | (13) |
| 1.3 | 18% | 75 | 3.4 | 1% | 75 | Glinsky | 79 | (14) |

**Supplemental Table 4**
COPA identified *MAOA* as markedly overexpressed in a subset of tumor samples in 15 out of 27 data sets available from Oncomine (gene rank, top 20%; fold change, >2; $p < 1 \times 10^{-4}$). Using the same statistical filters, MAOA exhibited a COPA score comparable to or higher than that of *ERG* in several data sets.

**Supplemental Methods**

*Analysis of Clinical Specimens.* Archival PCa specimens of defined Gleason grades were obtained as described in Methods. These archival collections were from a patient population that ranged in age from 59-84 (mean=73). None of the patients had received any hormonal or radiation therapy prior to radical prostatectomy or core biopsy. All cases of defined Gleason grades were selected for IHC analysis by a pathologist from the archived collections referred to above.

Formalin-fixed paraffin-embedded (FFPE) specimens were stained with antibodies specific for MAOA (1:100) (H-70, Santa Cruz), E-cadherin (1:50) (24E10, Cell Signaling), Vimentin (1:500) (V9, Santa Cruz), HIF1α (1:30) (H1alpha67, Novus Biologicals), VEGF-A (1:40) (A-20, Santa Cruz), FoxO1 (1:50) (2H8.2, Millipore), pFoxO1 (Thr24) (1:50) (Millipore), and Twist1 (1:80) (Sigma-Aldrich) following our published protocol (15) with minor modifications. The scoring system used was a semi-quantitative method (16) that is based upon the proportion of tumor cells stained quantity (q) and the staining intensity (I) to obtain a final score (Q) defined as the product of I X q. The scoring system for q was: 0=negative, 1=1-9% positive, 2=10-39% positive, 3=40-69% positive, 4=70-100% positive cells. The scoring system for I was: 0=negative, 1=low, 2=moderate, 3=intense immunostaining. All scoring was performed by a pathologist.

*Cells and Reagents.* Human PCa 22Rv1 cell line was obtained from American Type Culture Collection (ATCC Manassas, VA). Human PCa LAPC-4 cell line was kindly provided by Dr. Michael Freeman (Cedars-Sinai Medical Center, Los Angeles, CA). Human *HIF1α*-, *FoxO1*- and *Twist1*-targeting shRNA lentiviral particles were purchased from Santa Cruz. Human *PHD1*, *PHD2*, *PHD3*, *PHD4* and non-targeting control siRNA were purchased from Santa Cruz. Human recombinant $VEGF_{165}$ protein was purchased from R&D Systems.

*Immunohistochemical Analysis of Tumor Xenograft and Mouse Primary Prostatic Tumor Specimens.* FFPE tumor xenograft specimens were stained with antibodies specific for Ki-67 (1:200) (SP6, Abcam), MAOA (1:100) (H-70, Santa Cruz), E-cadherin (1:50) (24E10, Cell Signaling), Vimentin (1:100) (V9, Santa Cruz), HIF1α (1:25) (54, BD Bioscience), VEGF-A (1:40) (A-20, Santa Cruz), and NRP1 (1:50) (C-19, Santa Cruz) following our published protocol (15) with minor modifications. Normal (wild-type) and neoplastic (9-month-old prostate-specific *Pten*-KO primary tumor) tissues of mouse dorsolateral prostatic lobes were stained with anti-MAOA antibody (1:100) (H-70, Santa Cruz) following our published protocol (15, 17) with minor modifications.

*Quantum Dot (QD) Labeling Analysis of Mouse Primary Prostatic Tumor Specimens.* The IHC staining protocol was modified for QD labeling as described previously (18). Normal (wild-type) and neoplastic (9-month-old prostate-specific *Pten*-KO primary tumor) tissues of mouse dorsolateral prostatic lobes were stained with anti-MAOA antibody (1:200) (H-70, Santa Cruz) by single QD labeling. Cell-based average of signal intensity counts were analyzed by inForm software.

*TUNEL Assay.* Cell death in PC-3 (vector and MAOA-overexpression) and LNCaP (shCon and shMAOA) cells were detected and analyzed by a fluorescence-based cell death detection kit (Roche) following the manufacturers' instructions.

*Immunoblot.* Primary antibodies used for immunoblots were as follows: MAOA (1:500) (H-70, Santa Cruz), E-cadherin (1:2000) (H-108, Santa Cruz; 24E10, Cell Signaling),

Vimentin (1:500) (V9, Santa Cruz), N-cadherin (1:500) (32/N, BD Biosciences; H-63, Santa Cruz), Twist1 (1:500) (Twist2C1a, Santa Cruz), HIF1α (1:1000) (54, BD Bioscience), hydroxy-HIF1α (Pro564) (1:1000) (D43B5, Cell Signaling), Lamin B1 (1:1000) (Cell Signaling), GAPDH (1:4000) (14C10, Cell Signaling), pAkt (Ser473) (1:2000) (D9E, Cell Signaling), Akt (1:1000) (Cell Signaling), pFoxO1 (Thr24) (1:1000) (Cell Signaling), FoxO1 (1:500) (H-128, Santa Cruz), FoxO1 (1:1000) (2H8.2, Millipore), NRP1 (1:500) (C-19, Santa Cruz), β-Actin (1:2000) (AC-15, Sigma-Aldrich), COX IV (1:1000) (3E11, Cell Signaling), Histone H3 (1:2000) (D1H2, Cell Signaling), Sema3A (1:500) (N-15, Santa Cruz), PTEN (1:500) (28H6, Santa Cruz), p53 (7F5, Cell Signaling) and ERβ (1:500) (H-150, Santa Cruz).

*Quantitative Real-Time PCR.* qPCR was conducted using SYBR Green PCR Master Mix and run with Applied Biosystems 7500 Fast Real-Time PCR System (Applied Biosystems). PCR conditions included an initial denaturation step of 3 min at 95°C, followed by 40 cycles of PCR consisting of 30 s at 95°C, 30 s at 60°C, and 40 s at 72°C. The PCR data were analyzed by $2^{-\Delta\Delta CT}$ method (19). All primer sequences used are as follows:

| | |
|---|---|
| *MAOA* | F: CTGATCGACTTGCTAAGCTAC<br>R: ATGCACTGGATGTAAAGCTTC |
| *E-cadherin* | F: TGCCCAGAAAATGAAAAAGG<br>R: GTGTATGTGGCAATGCGTTC |
| *Vimentin* | F: GAGAACTTTGCCGTTGAAGC<br>R: GCTTCCTGTAGGTGGCAATC |
| *N-cadherin* | F: ACAGTGGCCACCTACAAAGG<br>R: CCGAGATGGGGTTGATAATG |
| *Snail2* | F: GGGGAGAAGCCTTTTTCTTG<br>R: TCCTCATGTTTGTGCAGGAG |
| *Twist1* | F: GGAGTCCGCAGTCTTACGAG<br>R: TCTGGAGGACCTGGTAGAGG |
| *VEGF-A* | F: GCTACTGCCATCCAATCGAG<br>R: CTCTCCTATGTGCTGGCCTT |
| *Glut1* | F: GTCACCATCCTGGAGCTGTT<br>R: GAAGGCCGTGTTGACGATAC |
| *HIF1α* | F: CAGAGCAGGAAAAGGAGTCA<br>R: AGTAGCTGCATGATCGTCTG |
| *PHD1* | F: AACATCGAGCCACTCTTTGAC<br>R: TCCTTGGCATCAAAATACCAG |
| *PHD2* | F: GAAAGCCATGGTTGCTTGTT<br>R: TTGCCTTCTGGAAAAATTCG |
| *PHD3* | F: ATCGACAGGCTGGTCCTCTA<br>R: CTTGGCATCCCAATTCTTGT |
| *PHD4* | F: AACATGGACCTTCGGGACTTC<br>R: TGTTCCGCACCAGCTCACT |
| *GAPDH* | F: GACAACAGCCTCAAGATCATCAG<br>R: ATGGCATGGACTGTGGTCATGAG |
| *β-Actin* | F: TTGTTACAGGAAGTCCCTTGCC<br>R: ATGCTATCACCTCCCCTGTGTG |

*Mutational Analysis of the Twist1 Promoter.* Site-directed mutagenesis was used to mutate the putative FoxO1-binding site identified in 1-kb *Twist1* promoter. Wild-type *Twist1* 1-kb-*luc* was used as the template. Mutagenesis was carried out using QuickChange XL Site-Directed Mutagenesis Kit (Agilent Technologies). The primers used for mutagenesis was forward 5'-CACTGCTGCCCCCGCGCTTTCCGCCTGC-3' (mutated nucleotides underscored). Mutated nucleotides were verified by DNA sequencing.

*Chromatin Immunoprecipitation Analysis and qPCR.* ChIP assay was used to determine the in vivo association of endogenous FoxO1 protein with *Twist1* promoter in both control and MAOA-overexpressing PC-3 cells by a SimpleChIP Enzymatic Chromatin IP Kit (Cell Signaling). Briefly, chromatin that was cross-linked with nuclear proteins, enzymatically digested with micrococcal nuclease and sonicated was immunoprecipitated with anti-FoxO1 antibody (H-128, Santa Cruz), which after pelleted with agarose beads and purified was subsequently subjected to qPCR with a pair of primers specifically targeting the *Twist1* promoter region that encompasses a FoxO1 response element. IgG included in the kit was used as a negative control for IP. A control primer set for *Twist1* exon1 was used as a negative control for PCR. Primer sequences for *Twist1* promoter were forward 5'-GGGAGGACGAATTGTTAGAC-3' and reverse 5'-GGGCGAGAGCTGCAGACTTG-3', and for *Twist1* exon1 were forward 5'-GGAGTCCGCAGTCTTACGAG-3' and reverse 5'-TCTGGAGGACCTGGTAGAGG-3'. Two percent of chromatin prior to immunoprecipitation was saved as input, and data were presented as the percent of input from three separate experiments.

**Supplemental References**


1. Taylor BS, Schultz N, Hieronymus H, Gopalan A, Xiao Y, Carver BS, Arora VK, Kaushik P, Cerami E, Reva B, et al. Integrative genomic profiling of human prostate cancer. *Cancer Cell.* 2010;18(1):11-22.
2. Varambally S, Yu J, Laxman B, Rhodes DR, Mehra R, Tomlins SA, Shah RB, Chandran U, Monzon FA, Becich MJ, et al. Integrative genomic and proteomic analysis of prostate cancer reveals signatures of metastatic progression. *Cancer Cell.* 2005;8(5):393-406.
3. Liu P, Ramachandran S, Ali Seyed M, Scharer CD, Laycock N, Dalton WB, Williams H, Karanam S, Datta MW, Jaye DL, et al. Sex-determining region Y box 4 is a transforming oncogene in human prostate cancer cells. *Cancer Res.* 2006;66(8):4011-9.
4. Holzbeierlein J, Lal P, LaTulippe E, Smith A, Satagopan J, Zhang L, Ryan C, Smith S, Scher H, Scardino P, et al. Gene expression analysis of human prostate carcinoma during hormonal therapy identifies androgen-responsive genes and mechanisms of therapy resistance. *Am J Pathol.* 2004;164(1):217-27.
5. Yu YP, Landsittel D, Jing L, Nelson J, Ren B, Liu L, McDonald C, Thomas R, Dhir R, Finkelstein S, et al. Gene expression alterations in prostate cancer predicting tumor aggression and preceding development of malignancy. *J Clin Oncol.* 2004;22(14):2790-9.
6. Tomlins SA, Mehra R, Rhodes DR, Cao X, Wang L, Dhanasekaran SM, Kalyana-Sundaram S, Wei JT, Rubin MA, Pienta KJ, et al. Integrative molecular concept modeling of prostate cancer progression. *Nat Genet.* 2007;39(1):41-51.
7. Best CJ, Gillespie JW, Yi Y, Chandramouli GV, Perlmutter MA, Gathright Y, Erickson HS, Georgevich L, Tangrea MA, Duray PH, et al. Molecular alterations in primary prostate cancer after androgen ablation therapy. *Clin Cancer Res.* 2005;11(19 Pt 1):6823-34.
8. Tamura K, Furihata M, Tsunoda T, Ashida S, Takata R, Obara W, Yoshioka H, Daigo Y, Nasu Y, Kumon H, et al. Molecular features of hormone-refractory prostate cancer cells by genome-wide gene expression profiles. *Cancer Res.* 2007;67(11):5117-25.
9. Magee JA, Araki T, Patil S, Ehrig T, True L, Humphrey PA, Catalona WJ, Watson MA, and Milbrandt J. Expression profiling reveals hepsin overexpression in prostate cancer. *Cancer Res.* 2001;61(15):5692-6.
10. Wallace TA, Prueitt RL, Yi M, Howe TM, Gillespie JW, Yfantis HG, Stephens RM, Caporaso NE, Loffredo CA, and Ambs S. Tumor immunobiological differences in prostate cancer between African-American and European-American men. *Cancer Res.* 2008;68(3):927-36.
11. LaTulippe E, Satagopan J, Smith A, Scher H, Scardino P, Reuter V, and Gerald WL. Comprehensive gene expression analysis of prostate cancer reveals distinct transcriptional programs associated with metastatic disease. *Cancer Res.* 2002;62(15):4499-506.
12. Vanaja DK, Cheville JC, Iturria SJ, and Young CY. Transcriptional silencing of zinc finger protein 185 identified by expression profiling is associated with prostate cancer progression. *Cancer Res.* 2003;63(14):3877-82.
13. Nanni S, Priolo C, Grasselli A, D'Eletto M, Merola R, Moretti F, Gallucci M, De Carli P, Sentinelli S, Cianciulli AM, et al. Epithelial-restricted gene profile of primary cultures from human prostate tumors: a molecular approach to predict clinical behavior of prostate cancer. *Mol Cancer Res.* 2006;4(2):79-92.

14. Glinsky GV, Glinskii AB, Stephenson AJ, Hoffman RM, and Gerald WL. Gene expression profiling predicts clinical outcome of prostate cancer. *J Clin Invest.* 2004;113(6):913-23.
15. Zhau HE, Odero-Marah V, Lue HW, Nomura T, Wang R, Chu G, Liu ZR, Zhou BP, Huang WC, and Chung LW. Epithelial to mesenchymal transition (EMT) in human prostate cancer: lessons learned from ARCaP model. *Clin Exp Metastasis.* 2008;25(6):601-10.
16. Nanni S, Benvenuti V, Grasselli A, Priolo C, Aiello A, Mattiussi S, Colussi C, Lirangi V, Illi B, D'Eletto M, et al. Endothelial NOS, estrogen receptor beta, and HIFs cooperate in the activation of a prognostic transcriptional pattern in aggressive human prostate cancer. *J Clin Invest.* 2009;119(5):1093-108.
17. Liao CP, Zhong C, Saribekyan G, Bading J, Park R, Conti PS, Moats R, Berns A, Shi W, Zhou Z, et al. Mouse models of prostate adenocarcinoma with the capacity to monitor spontaneous carcinogenesis by bioluminescence or fluorescence. *Cancer Res.* 2007;67(15):7525-33.
18. Hu P, Chu GC, Zhu G, Yang H, Luthringer D, Prins G, Habib F, Wang Y, Wang R, Chung LW, et al. Multiplexed quantum dot labeling of activated c-Met signaling in castration-resistant human prostate cancer. *PLoS One.* 2011;6(12):e28670.
19. Livak KJ, and Schmittgen TD. Analysis of relative gene expression data using real-time quantitative PCR and the 2(-Delta Delta C(T)) Method. *Methods.* 2001;25(4):402-8.